

## ORIGINAL ARTICLE

# Non-invasive short-term assessment of retinoids effects on human skin *in vivo* using multiphoton microscopy

E. Tancrede-Bohin,<sup>1,2,\*</sup> T. Baldeweck,<sup>3</sup> E. Decencière,<sup>4</sup> S. Brizion,<sup>3</sup> S. Victorin,<sup>1</sup> N. Parent,<sup>1</sup> J. Faugere,<sup>3</sup> L. Souverain,<sup>3</sup> M. Bagot,<sup>2</sup> A-M. Pena<sup>3</sup>

<sup>1</sup>L'Oréal Research and Innovation, Paris, France

<sup>2</sup>Department of Dermatology, Saint-Louis Hospital, Paris, France

<sup>3</sup>L'Oréal Research and Innovation, Aulnay-sous-Bois, France

<sup>4</sup>Centre de Morphologie Mathématique, Mathématiques et Systèmes, MINES ParisTech, Fontainebleau, France

\*Correspondence: E. Tancrede-Bohin. E-mail: etancrede@rd.loreal.com

## Abstract

**Background** The occlusive patch test developed for assessing topical retinoids activity in human skin has been extended as a short-term screening protocol for anti-ageing agents. In this model, biopsies are performed at the end of the occlusion period for morphological and immuno-histochemistry analysis. Multiphoton microscopy is a recent non-invasive imaging technique that combined with image processing tools allows the *in vivo* quantification of human skin modifications.

**Objective** To validate with gold standards of anti-ageing that are retinoids, the relevance of multiphoton microscopy for kinetic and quantitative assessment in this model.

**Methods** Twenty women, aged 50–65 years, were enrolled. Retinol 0.3% (RO) and Retinoic acid 0.025% (RA) were applied to the dorsal photo-damaged side of their forearm under occlusive patches for 12 days. A patch alone was applied to a third area as control. Evaluation was performed at day D0, D12 (end of treatment), D18 and D32 using multiphoton microscopy. Epidermal thickness, normalized area of the dermal-epidermal junction (DEJ) and melanin density were estimated using 3D image processing tools.

**Results** Main significant results are:

- 1 Epidermal thickening at D12, D18 and D32 with RO and at D12, D18 with RA vs. baseline and vs. control.
- 2 Increased DEJ undulation at D32 with RO and at D12 with RA vs. baseline and vs. control.
- 3 Decreased melanin content with RO (at D12 and D18 vs. baseline and at D32 vs. baseline and vs. control) and with RA (at D12 vs. baseline).

**Conclusions** This study shows that multiphoton microscopy associated to specific 3D image processing tools allows cutaneous effects induced by topical retinoids in this *in vivo* model to be non-invasively detected, quantified and followed over time. This innovative approach could be applied to the evaluation of other active compounds.

Received: 9 April 2014; Accepted: 25 June 2014

## Conflicts of interest

E. Tancrede-Bohin, T. Baldeweck, S. Brizion, S. Victorin, N. Parent, J. Faugere, L. Souverain, A-M. Pena are employees of L'Oréal Research and Innovation who supported the study. One of the studied products Retinol is provided by the company but is used as gold standard, the objective of the study being validating an innovative method for evidencing its known effect. E. Decencière is one of the inventors of the patented 3D image processing tools used in this study. M. Bagot has no conflict of interest.

## Funding source

The study conducted herein was supported by L'Oréal Research and Innovation.

## Introduction

Topical retinoids are widely used in dermatology for their management of acne and ageing, and their effects on human skin have been extensively studied. In 1993, Griffiths *et al.* developed an occlusive patch test for assessing topical retinoid action *in vivo* in human skin,<sup>1</sup> showing that application of topical all-trans retinoic acid (RA) under occlusion for 4 days caused epidermal and granular layer thickening, *stratum corneum* (SC) compaction and increased glycosaminoglycan deposition. In 1995, Kang *et al.* showed that in this model, retinol (RO) also induced epidermal thickening and enhanced the expression of CRABP II and CRBP mRNAs and proteins, similar to RA.<sup>2</sup> This occlusive patch test has then been extended as a short-term screening protocol for photo-ageing repair agents, using fibrillin-1 as a reporter molecule.<sup>3,4</sup> In this model, biopsies are required at the end of the occlusion period for assessing morphological or immunohistochemical changes.

Multiphoton microscopy is a recent non-invasive skin imaging technique that allows the human skin 3D structure to be characterized *in vivo* with sub- $\mu\text{m}$  resolution.<sup>5</sup> This technique advantageously provides complementary modalities, such as two-photon excited fluorescence (2PEF) and second harmonic generation (SHG). In combination with endogenous contrast sources, these modalities allow tissues to be imaged under natural, non-invasive, physiological conditions. In the skin, 2PEF signals are emitted by endogenous chromophores such as NAD(P)H, flavins, keratin, melanin or elastin, whereas SHG signals, obtained from dense, non-centrosymmetrical and ordered macromolecular structures, reveal the fibrillar collagen.<sup>5–9</sup> *In vivo* multiphoton microscopy has already been applied to the study of skin ageing,<sup>10,11</sup> dermatological disorders and melanoma,<sup>12,13</sup> i.e. seeming a versatile tool to both cosmetic and pharmaceutical researchers.<sup>14</sup>

We recently developed 3D image processing tools for multiphoton images of human skin<sup>15–18</sup> that allow us to automatically segment the different skin layers and extract several quantitative parameters characterizing skin in terms of morphology, density and organization. For example, the different skin layers thickness can be quantified, as well as the melanin density or the shape of the dermal-epidermal junction (DEJ).

Compared to other non-invasive skin imaging techniques such as ultrasound (lack of resolution), optical coherence tomography (OCT) or confocal microscopy (lack of specificity for melanin detection), multiphoton microscopy offers the best compromise to characterize both melanin<sup>15</sup> and epidermis morphology.<sup>18</sup> Melanin visualization in confocal microscopy is based on its higher reflectivity, but cellular membranes and corneocytes can exhibit similar reflection signals. Concerning skin morphology (epidermal thickness, DEJ shape), OCT has a wider field of view, but presents low con-

trast between epidermis and dermis leading to a difficult DEJ detection. Conversely, in multiphoton microscopy, collagen fibres create specific SHG signals that allow locating very precisely the DEJ.

The aim of this study was to assess whether *in vivo* multiphoton microscopy could be used to evaluate the activity of anti-photo-ageing agents in the short-term screening protocol, thus overcoming the necessity of invasive biopsies.

## Materials and methods

### Subjects and treatment

This study involved 20 healthy female volunteers aged 50–65 years with a dorsal forearm skin colour determined by the Individual Typological Angle (ITA) value comprised between  $10^\circ$  and  $41^\circ$  (ITA group III/IV).<sup>19,20</sup> Two products, Retinol 0.3% (RO, Retinol 0.3<sup>®</sup>, SkinCeuticals, Inc., Garland, TX, United States) and all-trans Retinoic acid 0.025% (RA, Retacnyl<sup>®</sup>, Galderma S.A., Lausanne, Switzerland) were applied separately under standard patch test chambers (IQ Ultra<sup>®</sup>, Chemotechnique Diagnostics, Malmö, Sweden) onto the dorsal photo-damaged side of the volunteer's forearm for 12 days, as previously described.<sup>3</sup> A third area was left untreated but was occluded as control. These three  $1\text{ cm}^2$  areas were identified by tracing on transparent plastic sheets (Monaderm, Monaco, Monaco) natural anatomic marks (external and internal forearm edges, ulna head, elbow fold) and also nevus on volunteers in a standardized position. This allows the same central region of the respective three areas to be re-analysed. Evaluations were performed at day D0, D12 (end of occlusion period), D18 and D32 using multiphoton imaging and colorimetric measurements. Possible cutaneous irritation was followed up by a dermatologist at each visit. The study was double blinded, i.e. both investigator and volunteers ignored the product nature (or control) on each of the three skin areas. Standard photographs for illustration purposes were taken at different times of the study, using a digital camera (*Nikon D80*, Nikon Corporation, Tokyo, Japan). Saint Louis Hospital Ethics Committee approved the study and all volunteers gave written, informed consent (EC reference 2012/05).

### Multiphoton imaging and 3D Image processing

Multiphoton imaging was performed with DermaInspect<sup>™</sup> (JenLab GmbH, Jena, Germany), as previously described.<sup>16</sup> A multiphoton 3D ( $x, y, z$ ) image of  $130 \times 130 \times 162\ \mu\text{m}^3$  volume corresponds to a stack of 70 *en face* images of  $511 \times 511$  pixels ( $0.255\ \mu\text{m}/\text{pixel}$ ) acquired with  $2.346\ \mu\text{m}$   $z$ -step. For each volunteer, two 3D images were acquired per condition in two adjacent regions of the dorsal forearm side. Each 3D image starts and ends respectively at  $-10\ \mu\text{m}$  above and  $150\ \mu\text{m}$  below the skin surface.

The 3D images were analysed using automatic 3D image processing tools we recently developed.<sup>16,18</sup> All the 3D voxels are used and computed to automatically separate the different skin layers, characterize the 3D DEJ shape and extract quantitative parameters on the different skin constituents and layers. Briefly, the first step of this image processing consists in a 3D automatic segmentation of the different imaged compartments (coupling medium, epidermis and superficial dermis) taking into account the real shape of skin surface and DEJ. In addition, for this study, a 3D epidermis segmentation was performed into two sub-layers: *stratum corneum* and living epidermis (LED).

The second step consists in extracting quantitative parameters in the segmented epidermal layers. The following parameters were studied: SC, LED and total epidermis thickness, normalized DEJ area and melanin density. The thickness parameter was measured along the  $z$  axis at each  $(x, y)$  position and the mean value of each layer (in  $\mu\text{m}$ ) was computed. The normalized area of DEJ is a generalization in 3D of the index of interdigitation described in two dimensions by Timar *et al.* on histological sections of human skin.<sup>21</sup> Since this parameter is a ratio between two areas (real DEJ area and area of its projection on a horizontal plane), it has no unit. The DEJ value is  $\geq 1$ : totally flat DEJ leads to a normalized area equal to 1 and more undulated one to a higher value. Melanin quantification was performed using a specific melanin detection procedure associating multiphoton microscopy and fluorescence lifetime imaging.<sup>15</sup> Melanin density corresponds to the ratio of the number of voxels ('3D pixels') occupied by melanin and the total number of voxels in the volume occupied by the living epidermis.

**Colorimetric measurements** Skin colour was determined by the Individual Typology Angle (ITA) values using a microflash spectrophotometer (Datacolor, Montreuil, France)<sup>19,20</sup> that was calibrated before each measurement. Measurements were performed under a particular care to ensure that the colorimeter was held perpendicular to the assessed area, and that minimal pressure was applied to avoid skin blanching.

### Statistical methods

A descriptive analysis was performed for each parameter by time and treatment using boxplots to represent the data evolution and variability. An inferential analysis was also performed using a linear mixed model for quantitative longitudinal data with repeated time, and with treatment, time, interaction treatment\*time as fixed effects and subject as random effect. Within and between treatment groups, comparisons were performed using contrasts.  $P$ -values were adjusted using the Benjamini–Hochberg correction for multiple comparison tests. All hypothesis tests comparing the treatments were performed using two-sided tests with  $\alpha = 0.05$  significance level. Analyses were performed using IBM<sup>®</sup> SPSS<sup>®</sup> Statistics20 (IBM, Armonk,

NY, United States) and SAS/STAT<sup>®</sup> (SAS, Cary, NC, United States).

Each comparison test with adjusted  $p$ -value was completed with effect size (ES) which represent the difference of means between groups compared to the variability of the phenomenon and gives an idea of the strength of the modifications observed between groups.

Interpreting ES as a small or strong effect requires a prior knowledge of the effect sizes of contrasts clearly relevant in the context. Accordingly, the ES's of morphologic parameters corresponding to well-documented modifications of skin ageing, including the parameters analysed in this study, were calculated, in another study dealing with photo-ageing<sup>18</sup>. In this previous study, comparing two age groups (18–25 years and 70–75 years), the data were acquired on the same anatomic zone (forearm), with the same image acquisition and processing methodology. ES of the contrasts between younger and older subjects of epidermal thickness, normalized DEJ area, elastic fibre density (related to elastosis), were 0.91, 1.17 and 1.37 respectively. In this process, elastosis was considered "very strong" as photo-ageing superimposed to chronological ageing, and DEJ flattening and epidermis thickening as "strong". Concerning melanin quantification, ES of the melanin density contrast between the dorsal and volar forearm side in the same population was 0.87 and was also considered as strong. Therefore, the criteria to classify the strength of the ES in the present study were: very strong:  $ES > 1.3$ ; strong:  $0.8 < ES < 1.3$ ; moderate:  $0.5 < ES < 0.8$ ; small:  $0.3 < ES < 0.5$ ; very small:  $0 < ES < 0.3$ ; no effect:  $ES = 0$ .

### Results

In this kinetic study, treated areas were investigated at D0 (before treatment), D12 (end of occlusion), D18 and D32. Illustrative *in vivo* multiphoton images of normal skin before treatment are presented in Fig. 1. In the following text, the results are given as mean  $\pm$  SE.

#### Quantification results obtained after 3D image processing of multiphoton images

**Retinoids effects on epidermis thickness [see Fig. 2(a)]** Before treatment, the mean SC thickness was  $20 \pm 1.5 \mu\text{m}$  (data not shown), not significantly different between the three areas. Occlusion or treatments had no significant effect on this parameter at all observation times. Therefore, modifications of total epidermis and living epidermis thickness were similar and only results on LED are shown. Before treatment, the  $50 \pm 2.3 \mu\text{m}$  mean thickness of LED showed no significant difference between the three areas, and remained unchanged under occlusion alone. On RO-treated areas, a statistically significant increase in mean LED thickness was shown at D12, D18 and D32 as compared to D0 and control, reaching  $70 \pm 4 \mu\text{m}$ ,  $74 \pm 5 \mu\text{m}$  and

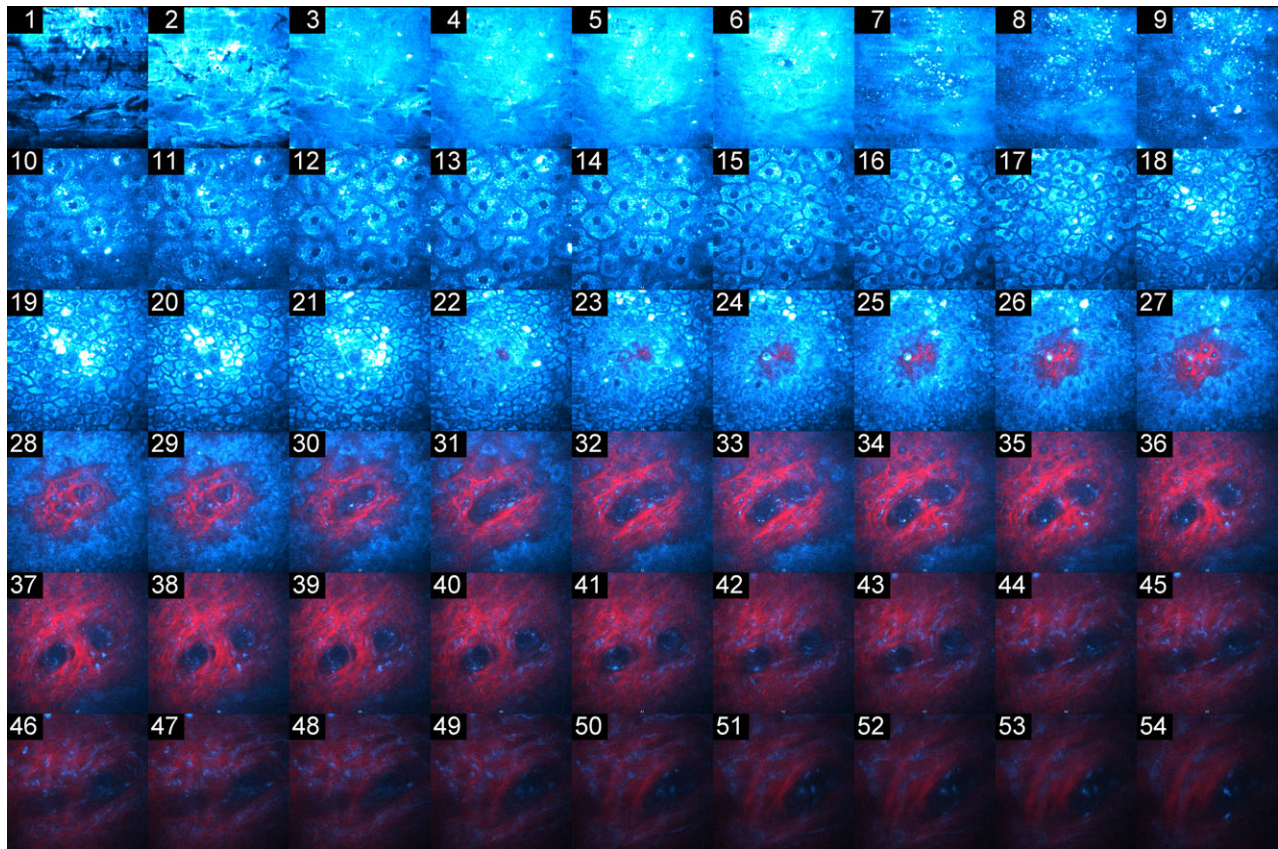


**Figure 1** *In vivo* multiphoton images of normal human skin before treatment. 3D image represented as a montage of a z-stack of combined 2PEF (cyan colour) / SHG (red colour) images (image number indicated at the top of each image). Images 1–3 correspond to *stratum corneum disjunctum* and images 4–8 to *stratum corneum compactum*. The keratinocytes in the *stratum granulosum* appear in image 9 and melanin distribution in the basal layers of the epidermis can be seen in images 18–27, with high melanin 2PEF intensity signal highlighted in white. Image 22 was acquired at the top of a dermal papilla level as indicated by the onset of collagen fibres of the dermis (red colour).

$64 \pm 3 \mu\text{m}$  respectively. It is important to notice that for 9/20 (D12) and 6/20 (D18) volunteers, the total epidermal thickness exceeded the maximum measurable thickness of  $150 \mu\text{m}$  in our imaging conditions ( $20 \mu\text{m}$ -SC,  $130 \mu\text{m}$ -LED,  $10 \mu\text{m}$  being acquired above the skin surface). For this reason, the mean LED thickness, calculated on 11 (D12) and 14 (D18) volunteers, was underestimated. On RA-treated areas, the increase in mean LED thickness was only statistically significant at D12 and D18 as compared to D0 and control, reaching  $61 \pm 3 \mu\text{m}$  and  $58 \pm 2 \mu\text{m}$  respectively. At D32, mean LED thickness was significantly higher on RO- as compared to RA-treated areas ( $p = 0.005$ ).

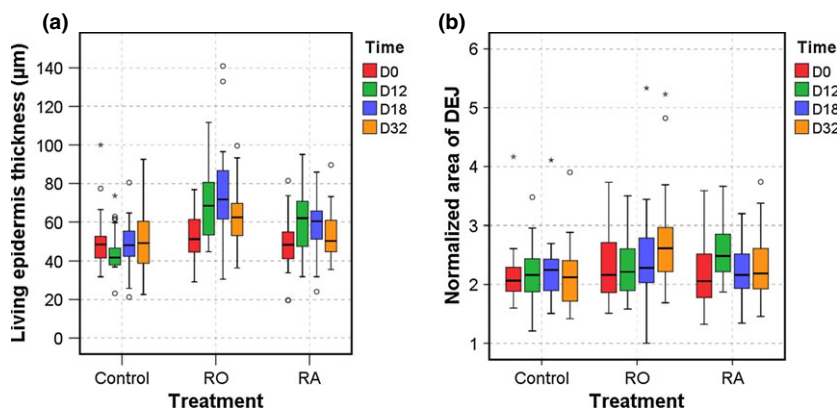
#### *Retinoids effects on dermal-epidermal junction [see Fig. 2(b)]*

Before treatment, the mean normalized area of the DEJ was  $2.2 \pm 0.1$  with no statistically significant difference between the three areas, occlusion alone bringing no significant effect on this parameter. On RO-treated areas, its mean value reached

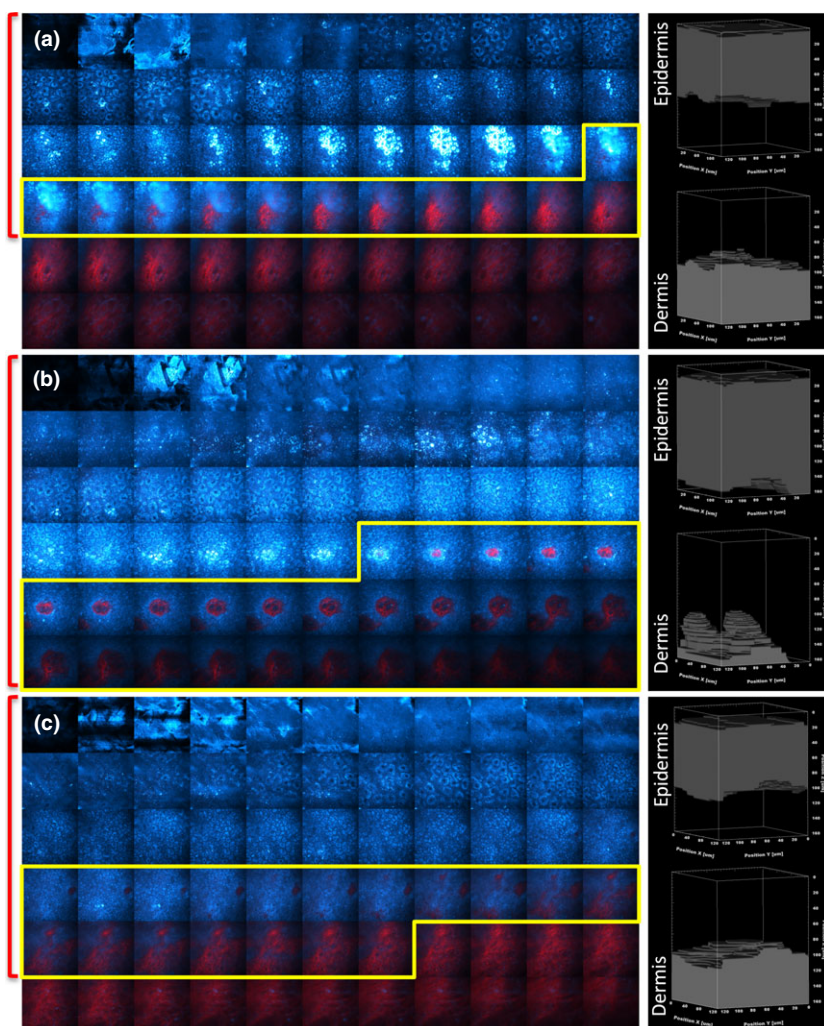
$2.7 \pm 0.1$  at D32, a statistically significant increase as compared to D0 and control. On RA-treated areas, the mean value reached  $2.6 \pm 0.1$  at D12, a statistically significant increase as compared to D0 and control. The comparison between RO and RA-treated areas at D32 showed that the DEJ was significantly more undulated on RO-treated areas as compared to RA-treated areas ( $p = 0.009$ ).

Figure 3 shows representative *in vivo* multiphoton images and 3D volume renderings of the segmented epidermal and dermal compartments at D32 for control (a), RO- (b) and RA-treated areas (c). Increase in DEJ undulation and epidermal thickness with retinoids treatment are clearly visible.

*Retinoids effects on melanin density (see Fig. 4)* Before treatment, mean melanin density in living epidermis was  $25 \pm 3\%$ , not significantly different between the three areas. Occlusion alone had no statistically significant effect on this parameter,



**Figure 2** Quantification results of retinoids effects on epidermal thickness and dermal-epidermal junction obtained with multiphoton microscopy. Change over time of (a) living epidermis thickness expressed in  $\mu\text{m}$ ; (b) normalized area of dermal-epidermal junction, no unit, a value equal to 1, correspond to a flat DEJ; the more the DEJ is undulated, the larger the parameter value. The data are expressed as boxplots with fences. The boxes contain 50% of the data; the intervals between the lower limit of the box and the lower inner fence contain 25%, and vice versa for the other 25%. — indicates the median that divides the population in two groups with equal numbers of data points;  $\circ$  the outliers and \* the extreme data points.



**Figure 3** *In vivo* multiphoton images of human skin at D32. 3D image represented as a montage of a z-stack of combined 2PEF (cyan colour) / SHG (red colour) images acquired at day D32 on Control (a), Retinol (RO) (b) and Retinoic acid (RA) (c)-treated areas. The epidermis is depicted as a red bracket and the dermal-epidermal junction as a yellow box. On the right, corresponding 3D volume renderings of the segmented epidermal and dermal compartments, obtained using the 3D automatic segmentation method, allow to visualize epidermis thickness and DEJ shape. The 3D volume renderings were created using Imaris<sup>®</sup>  $\times 64$ , 7.7.0, Bitplane AG, Zürich, Switzerland.

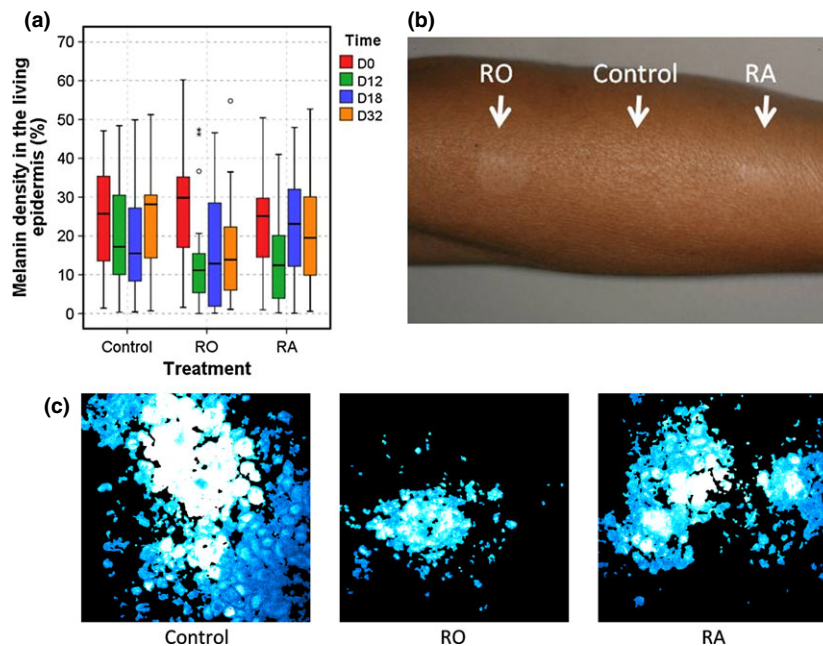


**Figure 4 Retinoids effects on melanin density.** At the top left, quantification of melanin density obtained with multiphoton microscopy in the living epidermis expressed in % for Control, Retinol (RO) and Retinoic acid (RA)-treated areas (a). The data are expressed as box-plots with fences. The boxes contain 50% of the data; the intervals between the lower limit of the box and the lower inner fence contain 25%, and vice versa for the other 25%. — indicates the median that divides the population in two groups with equal numbers of data points; ° the outliers and \* the extreme data points. At the top right, standard photography of the dorsal side of the left forearm of a volunteer showing the RO, Control and RA-treated areas showing a clear whitening of the skin on RO-treated area and a more discreet whitening on the RA-treated area (b). At the bottom, melanin masks obtained after image processing of 2PEF raw images at the basal layer, on the Control, RO and RA-treated areas (c) at D32.

although a slight decrease was observed at D12 (effect of occlusion). On RO-treated areas, mean melanin density was  $14 \pm 3\%$ ,  $16 \pm 3\%$  and  $16 \pm 2\%$  at D12, D18 and D32, respectively. Such a decrease was statistically significant as compared to baseline at all-time points and at D32 as compared to control. On RA-treated areas, the decrease in melanin density was only statistically significant at D12 ( $14 \pm 2\%$ ) as compared to baseline. At D32, a more pronounced decrease in melanin density was observed on RO- as compared to RA-treated areas ( $p = 0.017$ ). In some subjects, visible skin whitening was observed on both retinoid-treated areas which correlates with the decrease in melanin density [see Fig. 4(b)]. Changes in melanin density are clearly visible on melanin masks obtained after image processing of 2PEF raw images at the basal layer in each condition at D32 [see Fig. 4(c)].

The % of variation of each parameter between retinoid-treated and baseline or control areas at each time point with the detail of their  $p$ -value and ES are presented in Table 1.

#### Results from colorimetric measurements

Before treatment, the mean ITA value was  $25 \pm 1^\circ$  with no statistically significant difference between the three areas. On con-

trol areas, an increase in mean ITA value was observed at D12 as compared to baseline ( $+12\%$ ,  $p < 0.001$ ). On RO-treated areas, a decrease in mean ITA value was shown at D18 as compared to baseline ( $-11\%$ ,  $p = 0.0012$ ) and at D12 and D18 as compared to control ( $-5\%$ ,  $p = 0.021$  and  $-15\%$ ,  $p < 0.001$ , respectively). On RA-treated areas, an increase in mean ITA value was observed at D12 as compared to baseline and control ( $+19\%$ ,  $p < 0.001$  in both cases) and also at D18 and D32 as compared to control ( $+13\%$ ,  $p = 0.001$  and  $+12\%$ ,  $p = 0.006$ , respectively).

#### Tolerance

Topical application of retinoids under occlusion for 12 days produced cutaneous irritation on 19 out of 20 RO-treated areas, and on 14 out of 20 RA-treated areas at D12 that resolved within a few days in all cases. Erythema and scaling, ranging from moderate to marked as judged by the dermatologist, were more pronounced on RO- than on RA-treated areas.

#### Discussion

The occlusive patch test initially developed for assessing the effects of topical retinoids on human skin,<sup>1</sup> has been extended as a short-term protocol for screening anti-photo-ageing agents.<sup>3,4</sup>

**Table 1** Main results of retinol and retinoic acid effects on epidermal parameters measured using multiphoton microscopy

QUANTITATIVE MEASUREMENT	Treatment	Statistics	D12		D18		D32	
			vs. baseline	vs. control	vs. baseline	vs. control	vs. baseline	vs control
LIVING EPIDERMIS THICKNESS	Retinol 0.3%	% variation	+33%	+53%	+41%	+53%	+23%	+24%
		p-value	<0.001	<0.001	<0.001	<0.001	0.004	0.013
		ES*	Strong	Very strong	Very strong	Very strong	Strong	Strong
	Retinoic acid 0.025%	% variation	+26%	+35%	+19%	+20%	+8%	+2%
		p-value	<0.001	<0.001	0.010	0.004	N.S.	N.S.
		ES*	Strong	Strong	Moderate	Strong	/	/
DEJ UNDULATION	Retinol 0.3%	% variation	-2%	+6%	+5%	+10%	+17%	+27%
		p-value	N.S.	N.S.	N.S.	N.S.	0.013	0.005
		ES*	/	/	/	/	Moderate	Strong
	Retinoic acid 0.025%	% variation	+26%	+20%	+3%	-1%	+7%	+5%
		p-value	0.005	0.027	N.S.	N.S.	N.S.	N.S.
		ES*	Strong	Moderate	/	/	/	/
MELANIN DENSITY	Retinol 0.3%	% variation	-50%	-26%	-44%	-15%	-45%	-34%
		p-value	<0.001	N.S.	0.007	0,087	<0.001	0.048
		ES*	Strong	/	Strong	Moderate	Strong	Moderate
	Retinoic acid 0.025%	% variation	-25%	-38%	+18%	-4%	-10%	-9%
		p-value	0.012	N.S.	N.S.	N.S.	N.S.	N.S.
		ES*	Moderate	/	/	/	/	/

Variations with time are presented in % vs. baseline and vs. control.

In this protocol, biopsies are performed at the end of the occlusion period for immuno-histochemical analysis, making assessments only possible immediately after occlusion.

Multiphoton microscopy, a recent *in vivo* skin imaging technique, enables a non-invasive assessment of dermatological/cosmetic products induced skin modifications throughout a study: before, during and after treatment.

Since this technology has emerged, only a few imaging processing methods have been developed to extract quantitative parameters on skin constituents. We developed the first 3D image processing tools for multiphoton images of human skin.<sup>16-18</sup> In this short-term screening study, effects of retinoids

were addressed using these tools at D0, D12 (end of treatment), D18 and D32. We showed that this method allows epidermal modifications induced by retinoids to be detected and quantified immediately after occlusion, but also over the post treatment period; it also allows specific *in vivo* melanin detection and quantification.<sup>15</sup>

Before treatment, our results on living epidermal thickness on the dorsal forearm side are in agreement with published data obtained with histology.<sup>22,23</sup> According to previous studies,<sup>1-3,24,25</sup> both RO and RA were shown to increase epidermal thickness after the occlusion period. At this end point, as previously discussed,<sup>1</sup> irritation-induced oedema could be responsible for epider-

mal thickening. Effectively, local irritation, a frequent side-effect of topical retinoids, was noted in 19 out of 20 RO-treated areas, and in 14 out of 20 RA-treated areas at D12, related to extensive occlusion procedure. Whatsoever, erythema and scaling resolved within a few days and can hardly account for the epidermal thickening observed at D32.

Additionally, multiphoton microscopy evidenced an increase in DEJ undulation with retinoid treatment, the effect of RO being, to our knowledge, a new finding.

Retinoid induced decrease in melanin content is also observed for the first time in such short-term protocol as revealed by multiphoton microscopy. Colorimetric data (ITA measurements) indicate slight skin lightening on control areas at D12 (occlusion effect) and on RA-treated areas at D12, D18 and D32. A decreased ITA value, which corresponds to a darker skin, was observed on RO-treated areas at D12 and D18, although visible whitening was seen in some cases. At these time points, this is probably due to the marked RO-induced irritation upon the L\* criterion that is influenced by pigmentation but also by scaling and erythema,<sup>26</sup> as shown in erythematous skin lesions of psoriasis.<sup>27</sup> We show here that multiphoton microscopy, which allows specific melanin detection and quantification, overcomes the known bias of colorimetric interferences induced by other constituents than melanin e.g. haemoglobin when evaluating cutaneous pigmentation.

For comparable concentrations, studies of the literature suggest that RA is more effective and irritant than RO, although there are no studies comparing them directly in this condition. In this study, beneficial effects on epidermal morphology and pigmentation on photo-damaged skin are more pronounced with RO than with RA which is probably due to the high concentration of RO used (0.3%), 12 times higher compared to that of RA (0.025%). For the same reason, local irritation was also more frequent and more intense with RO than with RA but resolved in both cases in a few days in all volunteers.

Multiphoton imaging on the skin is limited to the epidermis and the superficial dermis with an imaging depth of around 150  $\mu\text{m}$  in our experimental conditions which corresponds to approximately 80  $\mu\text{m}$  of dermis in a normal untreated skin. Hence, the approach of comparing signals in the superficial dermis in this study, into which epidermal thickness increased drastically and exceeded 150  $\mu\text{m}$  at some time points, was not possible. Moreover, although increased fibrillin1 has been shown as reporter molecule for dermal repair in short-term protocols<sup>3,4</sup> with retinoids, we believe that morphological changes in the dermis that could be addressed with this technique are not likely to be observed in such short period of treatment. Possible effect of retinoids in the superficial dermal structure using this technique will be further addressed in a long-term study with open applications and using image processing tools that allow comparison of an equivalent 3D volume of dermis between treated and control skin.

In conclusion, this study shows that short-term protocol in combination with non-invasive *in vivo* multiphoton microscopy allows epidermal effects induced by retinoids, including melanin content, to be accurately detected and quantified over time. We report here the first application of innovative specific 3D quantification tools for multiphoton images to the evaluation of a cutaneous treatment. This new approach could be generalized to the evaluation of other molecules.

### Acknowledgement

The authors gratefully acknowledge R. Dalmaschio for her help for manuscript preparation.

### References

- 1 Griffiths CEM, Finkel LJ, Tranfaglia MG *et al.* An *in vivo* experimental model for effects of topical retinoic acid in human skin. *Br J Dermatol* 1993; **129**: 389–394.
- 2 Kang S, Duell EA, Fisher GJ *et al.* Application of retinol to human skin *in vivo* induces epidermal hyperplasia and cellular retinoid binding proteins characteristic of retinoic acid but without measurable retinoic acid levels or irritation. *J Invest Dermatol* 1995; **105**: 549–556.
- 3 Watson REB, Craven NM, Kang S *et al.* A short-term screening protocol, using fibrillin-1 as a reporter molecule, for photoaging repair agents. *J Invest Dermatol* 2001; **116**: 672–678.
- 4 Watson REB, Long SP, Bowden JJ *et al.* Repair of photoaged dermal matrix by topical application of a cosmetic ‘antiaging’ product. *Br J Dermatol* 2008; **158**: 472–477.
- 5 König K, Riemann I. High-resolution multiphoton tomography of human skin with subcellular spatial resolution and picosecond time resolution. *J Biomed Opt* 2003; **8**: 432–439.
- 6 Masters BR, So PTC, Gratton E. Multiphoton excitation fluorescence microscopy and spectroscopy of *in vivo* human skin. *Biophys J* 1997; **72**: 2405–2412.
- 7 Campagnola PJ, Millard AC, Terasaki M *et al.* Three-dimensional high-resolution second-harmonic generation imaging of endogenous structural proteins in biological tissues. *Biophys J* 2002; **82**: 493–508.
- 8 Zipfel WR, Williams RM, Christiet R *et al.* Live tissue intrinsic emission microscopy using multiphoton-excited native fluorescence and second harmonic generation. *Proc Natl Acad Sci USA* 2003; **100**: 7075–7080.
- 9 Pena A-M, Strupler M, Boulesteix T *et al.* Spectroscopic analysis of keratin endogenous signal for skin multiphoton microscopy. *Opt Express* 2005; **13**: 6268–6274; erratum: 13(17)6667.
- 10 Koehler MJ, König K, Elsner P *et al.* *In vivo* assessment of human skin aging by multiphoton laser scanning tomography. *Opt Lett* 2006; **31**: 2879–2881.
- 11 Koehler MJ, Preller A, Kindler N *et al.* Intrinsic, solar and sunbed-induced skin aging measured *in vivo* by multiphoton laser tomography and biophysical methods. *Skin Res Technol* 2009; **15**: 357–363.
- 12 Dimitrow E, Riemann I, Ehlers A *et al.* Spectral fluorescence lifetime detection and selective melanin imaging by multiphoton laser tomography for melanoma diagnosis. *Exp Dermatol* 2009; **18**: 509–515.
- 13 Paoli J, Smedh M, Ericson MB. Multiphoton Laser Scanning Microscopy—A Novel Diagnostic Method for Superficial Skin Cancers 25. *Semin Cutan Med Surg* 2009; **28**: 190–195.
- 14 König K, Ehlers A, Stracke F *et al.* *In vivo* drug screening in human skin using femtosecond laser multiphoton tomography. *Skin Pharmacol Physiol* 2006; **19**: 78–88.
- 15 Pena A-M, Baldebeck T, Tancrede E *et al.* Non-invasive method for specific 3D detection, visualization and/or quantification of an endogenous



- fluorophore such as melanin in a biological tissue. (French patent FR2982369 filed November 8, International publication number WO2013068943). 2011.
- 16 Ait El Madani H, Tancredi-Bohin E, Bensussan A *et al.* *In vivo* multiphoton imaging of human skin: assessment of topical corticosteroid-induced epidermis atrophy and depigmentation. *J Biomed Opt* 2012; **17**: 026009.
  - 17 Baldeweck T, Tancredi E, Dokladal P *et al.* *In vivo* multiphoton microscopy associated to 3D image processing for human skin characterization. Progress in Biomedical Optics and Imaging - Proceedings of SPIE **8226**. 2012. San Francisco, CA. Multiphoton Microscopy in the Biomedical Sciences XII. 22-1-2012.
  - 18 Decencière E, Tancredi-Bohin E, Dokladal P *et al.* Automatic 3D segmentation of multiphoton images: a key step for the quantification of human skin. *Skin Res Technol* 2013; **19**: 115–124.
  - 19 Chardon AF, Cretois IF, Hourseau C. Skin colour typology and sun-tanning pathways. *Int J Cosmet Sci* 1991; **13**: 191–208.
  - 20 Del Bino S, Sok J, Bessac E *et al.* Relationship between skin response to ultraviolet exposure and skin color type. *Pigm Cell Res* 2006; **19**: 606–614.
  - 21 Timár F, Soós Gy, Szende B *et al.* Interdigitation index - A parameter for differentiating between young and older skin specimens. *Skin Res Technol* 2000; **6**: 17–20.
  - 22 Sandby-Moller J, Poulsen T, Wulf HC. Epidermal thickness at different body sites: relationship to age, gender, pigmentation, blood content, skin type and smoking habits. *Acta Derm -Venereol* 2003; **83**: 410–413.
  - 23 Querleux B, Baldeweck T, Diridollou S *et al.* Skin from various ethnic origins and aging: an *in vivo* cross-sectional multimodality imaging study. *Skin Res Technol* 2009; **15**: 306–313.
  - 24 Fisher GJ, Esmann J, Griffiths CEM *et al.* Cellular, immunologic and biochemical characterization of topical retinoic acid-treated human skin. *J Invest Dermatol* 1991; **96**: 699–707.
  - 25 Rosenthal DS, Griffiths CEM, Yuspa SH *et al.* Acute or chronic topical retinoic acid treatment of human skin *in vivo* alters the expression of epidermal transglutaminase, loricrin, involucrin, filaggrin, and keratins 6 and 13 but not keratins 1, 10, and 14. *J Invest Dermatol* 1992; **98**: 343–350.
  - 26 Park SB, Sue DH, Youn JI. A long-term time course of colorimetric evaluation of ultraviolet light- induced skin reactions. *Clin Exp Dermatol* 1999; **24**: 315–320.
  - 27 Takiwaki H, Serup J. Measurement of color parameters of psoriatic plaques by narrow-band reflectance spectrophotometry and tristimulus colorimetry. *Skin Pharmacol* 1994; **7**: 145–150.